

Dielectric relaxation in Yb-doped SrZrO₃

This article has been downloaded from IOPscience. Please scroll down to see the full text article.

2004 J. Phys.: Condens. Matter 16 4971

(<http://iopscience.iop.org/0953-8984/16/28/017>)

View [the table of contents for this issue](#), or go to the [journal homepage](#) for more

Download details:

IP Address: 129.252.86.83

The article was downloaded on 27/05/2010 at 15:59

Please note that [terms and conditions apply](#).

Dielectric relaxation in Yb-doped SrZrO₃

O Kamishima¹, Y Abe¹, T Ishii², J Kawamura¹ and T Hattori¹

¹ Institute of Multidisciplinary Research for Advanced Materials, Tohoku University, Sendai 980-8577, Japan

² Faculty of Engineering, Okayama University, Okayama 700-8530, Japan

E-mail: o.kami@tagen.tohoku.ac.jp

Received 25 February 2004

Published 2 July 2004

Online at stacks.iop.org/JPhysCM/16/4971

doi:10.1088/0953-8984/16/28/017

Abstract

The dielectric constant of the proton conductor SrZr_{1-x}Yb_xO₃ ($x = 0-0.1$) was measured as a function of temperature and frequency. Two well-defined relaxation peaks were observed in SrZrO₃ doped with more than 1 mol% of Yb. The assignment of the two dielectric relaxations is discussed in terms of IR spectra and by free energy calculation for a miscibility of dopant Yb ions. The Yb concentration dependence of the relaxation strength of the two dielectric relaxations is in agreement with the results calculated from the free energy. The two relaxations can be assigned to a reorientation of a single Yb–OH dipole and of Yb–OH dipoles associated with Yb-clusters. The attractive energy for Yb-clustering in SrZrO₃ is evaluated at about -85 meV.

1. Introduction

When some perovskite-type oxides A²⁺B⁴⁺O₃ are doped with a few mol% trivalent cations at a quadrivalent B site and annealed in moisturized air, protons are incorporated into the crystals in order to keep the charge neutrality condition. By this treatment, some oxides (SrCeO₃, SrZrO₃, BaCeO₃, BaZrO₃, etc) exhibit considerably high protonic conductivity [1–6]. The protons migrate by hopping from one position close to an oxygen ion to another. These proton conducting oxides have been studied for applications to various devices such as fuel cells and hydrogen sensors operated at high temperatures. The fundamental scientific interest has increased in recent years mainly concerning the proton diffusion mechanism.

Regarding the local structure around the dopant ions, it was found in EXAFS measurements for SrZrO₃:Yb that the nearest Yb–O bonds consisted of two large different distances (1.96 and 2.18 Å) [7]. This result implied that the Yb dopants were displaced about 0.1 Å from the central position of the [YbO₆]-octahedron [7]. Since undoped-SrZrO₃ belongs to the space group *Pnma* ($Z = 4$, orthorhombic) below ~ 1000 K [8, 9], the Zr ions locate at the centre of the [ZrO₆]-octahedron. The charge balance with oxygen is maintained to be neutral in

the O-octahedron including the Zr ions. In the case of the [YbO₆]-octahedron, however, a significant polarization would appear locally because of the different valence charge of Yb³⁺ and Zr⁴⁺, and the off-centred location. The proton diffusion may be affected by such a local polarization in the vicinity of the Yb dopants.

Based on the neutron quasielastic scattering for SrCeO₃:Yb, which belongs to the same group of perovskite-type proton conductors, Hempelmann and Karmonik [10] suggested that the proton diffusion process was characterized as a combination of trapping and escape events. The proton traps were suggested to associate with the dopant Yb ions. Ishii and Ichigozaki [11] theoretically investigated relaxation modes by proton hopping in a perovskite lattice. They discussed impurity relaxation modes when the proton has a deep potential energy as the trapping state, and suggested that such a deep potential may not exist. In contrast to the dopant–proton trapping description, Kreuer *et al* [12] suggested that an increase in activation energy for protons with increasing dopant concentration would be related to the general increase of the oxygen basicity rather than proton–dopant association. Therefore, the dynamics of the proton as an interaction between proton and dopant is not fully understood.

If the proton is trapped by oxygen around the Yb ion, a dipole should be made locally (i.e. effectively negative charged Yb and positive charged proton). Dipole relaxation was experimentally recognized to exist in perovskite-type proton conductors by dielectric and mechanical relaxation measurements [13–16]. The H⁺–Yb interaction will be seen by measuring the Yb concentration dependence of the dipoles. In this paper, the frequency and temperature dependence of the complex dielectric constant was investigated for a proton conductor SrZrO₃:Yb with varying Yb concentration.

2. Experimental details

The polycrystals SrZr_{1-x}Yb_xO₃ ($x = 0.0, 0.01, 0.02, 0.03, 0.04, 0.05$ and 0.10) were grown by the floating zone method using an Xe-arc imaging furnace, and cut into cylindrical shape with 2.5–3.0 mm in diameter and 2.0–2.7 mm in thickness. The crystals were characterized as having the orthorhombic perovskite structure by x-ray powder diffraction; the samples were prepared by crushing some of the crystals [9]. The reliability of the Yb concentration ‘ x ’ against the nominal composition was within ± 0.005 , which was confirmed by an x-ray fluorescence analysis using an SEA2010 (Seiko Instruments Co.). Hence, in this paper x is described at the nominal composition. Sample crystals were annealed at 600 °C for 24 h in wet air, i.e. in water vapour pressure (0.69 atm). In order to check the amount of protons in the samples, IR absorption spectra were measured at room temperature by an FT-IR spectrometer (Parkin Elmer Spectrum GX) in the wavenumber range of 1500–4500 cm⁻¹.

The samples with cylindrical shape were mounted in a cell with gold coated electrodes (13 mm in diameter) and held under spring tension. Flowing gas (N₂ and O₂), humidified by bubbling through water at ambient temperature via a glass tube, was passed to the cell. The complex impedance was measured by means of a frequency response analyser (Solartoron 1260) in the frequency range of 0.1 Hz–1 MHz with logarithmic stepping and with an oscillation voltage <1 V. Since the current was so weak in the range of 0.1 Hz–1 kHz, a current amplifier (Keithley428) was also used. Impedance spectra were collected at temperatures between 50 and 300 °C with a step of 50 °C.

3. Results

Figure 1 shows the frequency dependence of the real (ϵ') and imaginary (ϵ'') parts of the complex dielectric constant $\epsilon^* = \epsilon' - i\epsilon''$ and the dielectric loss angle $\tan \delta (= \epsilon''/\epsilon')$. In

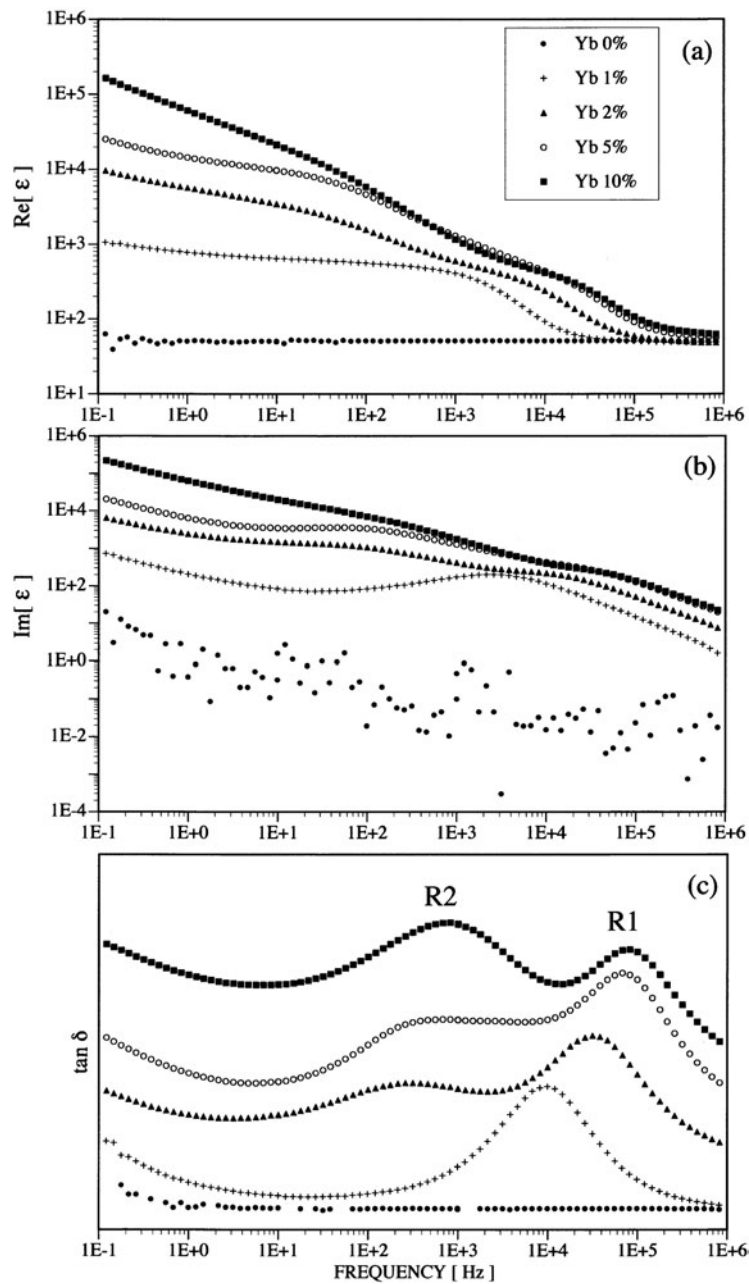


Figure 1. The frequency dependence of (a) ϵ' , (b) ϵ'' and (c) $\tan \delta$ of SrZr_{1-x}Yb_xO₃ of ($x = 0.0, 0.01, 0.02, 0.05$ and 0.10) at 150°C .

the case of undoped-SrZrO₃, dielectric relaxation was not observed. Since the current signal was too weak to measure, the values of ϵ'' of Yb 0% were scattered. On the other hand, a dielectric relaxation appeared at around 10 kHz in SrZr_{0.99}Yb_{0.01}O₃ (Yb 1%). The presence of dopant Yb plays a crucial role for the dielectric relaxation. The frequency region of the relaxation peak is in agreement with the one reported by Zimmermann *et al* [14]. On doping

a further amount of Yb, another dielectric loss peak was observed, as shown in figure 1(c). Two relaxation peaks were also observed in Nd-doped BaCeO₃ by a mechanical relaxation technique [15] and in Yb-doped SrCeO₃ by dielectric relaxation [16]. The relaxation in the higher frequency side is defined as relaxation 1 (R1), and that in the lower frequency side is defined as relaxation 2 (R2).

Both the real and imaginary parts of the dielectric constant were evaluated by nonlinear least-squares fitting with the following formula based on the Havriliak–Negami form [17]:

$$\varepsilon^* = \varepsilon_\infty + \sigma_0(i\omega)^{-\gamma} + \frac{\Delta\varepsilon_1}{[1 + (i\omega\tau_1)^{\alpha_1}]^{\beta_1}} + \frac{\Delta\varepsilon_2}{[1 + (i\omega\tau_2)^{\alpha_2}]^{\beta_2}}. \quad (1)$$

This reduces to the Davidson–Cole form when $\alpha = 1$, the Cole–Cole form when $\beta = 1$, or the Debye form when $\alpha = \beta = 1$. The magnitude of $\Delta\varepsilon$ is approximately proportional to the product of the size and number of the dipoles, so it is called a relaxation strength. The conduction loss contribution $\sigma_0(i\omega)^{-\gamma}$ ($\gamma = 1$ is ideally used) occurs due to the free carrier [18]. The parameters used for the best fitting are ε_∞ , $\Delta\varepsilon$, τ , α , β , σ_0 and γ . Figure 2 shows one of the best fitting results (solid curve) compared with experimental data (full circle). The dotted curve shows the conduction loss with ε_∞ by the first and second terms of equation (1). The two types of dashed curves represent the dielectric relaxations R1 and R2. The activation energy E_a was estimated by an Arrhenius plot of the relaxation time τ against the reciprocal temperature, i.e. $\tau = \tau_0 \exp(E_a/k_B T)$, as shown in figure 3. The Yb concentration dependence of each activation energy and the relaxation strength $\Delta\varepsilon$ are shown in figures 4(a) and (b), respectively. The response of R1 is faster in view of the relaxation time, while its activation energy is smaller than R2. With an increase in Yb concentration, the activation energies of the R1 and R2 tend to approach the same value. On the other hand, the relaxation strength $\Delta\varepsilon$ shows a quite different dependence on the Yb concentration between R1 and R2. The magnitude $\Delta\varepsilon$ of R1 almost decreases with an increase in Yb, and that of R2 dramatically increases.

4. Discussion

Three types of carriers (proton, oxygen vacancy (V_O) and hole) have been known for perovskite-type proton conductors. Since protons and oxygen vacancies occupy the vicinity of either Yb or Zr, the following four types of dipoles can be considered except for holes: (a) Yb–OH, (b) Yb–V_O, (c) Zr–OH and (d) Zr–V_O. It has been reported that the transport number of the oxygen vacancy was close to 0 below 600 °C for BaCe_{0.9}Yb_{0.1}O₃ [19], which belongs to the same group of perovskite-type proton conductors. It is concluded that dipole reorientation by oxygen hopping is a negligible contribution in the temperature range from 50 to 300 °C. All the present activation energies are nearly consistent with the value (0.58(9) eV) determined by the proton diffusivity [20]. In order to estimate the amount of the protons, IR absorption measurements were carried out for the various Yb concentration samples; the results are shown in figure 5. There is a weak band at around 1800 cm⁻¹, and two large absorption bands at around 2500 and 3100 cm⁻¹ (marked by A, B and C). These peak positions of the bands are in agreement with those of previous studies on perovskite-type proton conductors [21, 22]. The positions hardly depend on the Yb concentration, but the –OH absorptions increase with an increase in Yb concentration. Therefore, (a) Yb–OH and (c) Zr–OH are the more possible sources of the observed dielectric relaxations.

The OH-stretching absorption was decomposed into three Gaussian bands. Figure 6(a) shows the Yb concentration dependence of the integrated intensities of the three Gaussian bands, indicating the population of protons at the three types of state. Figure 6(b) also shows the Yb concentration dependence of the integrated intensity ratios A/C and B/C. It is found

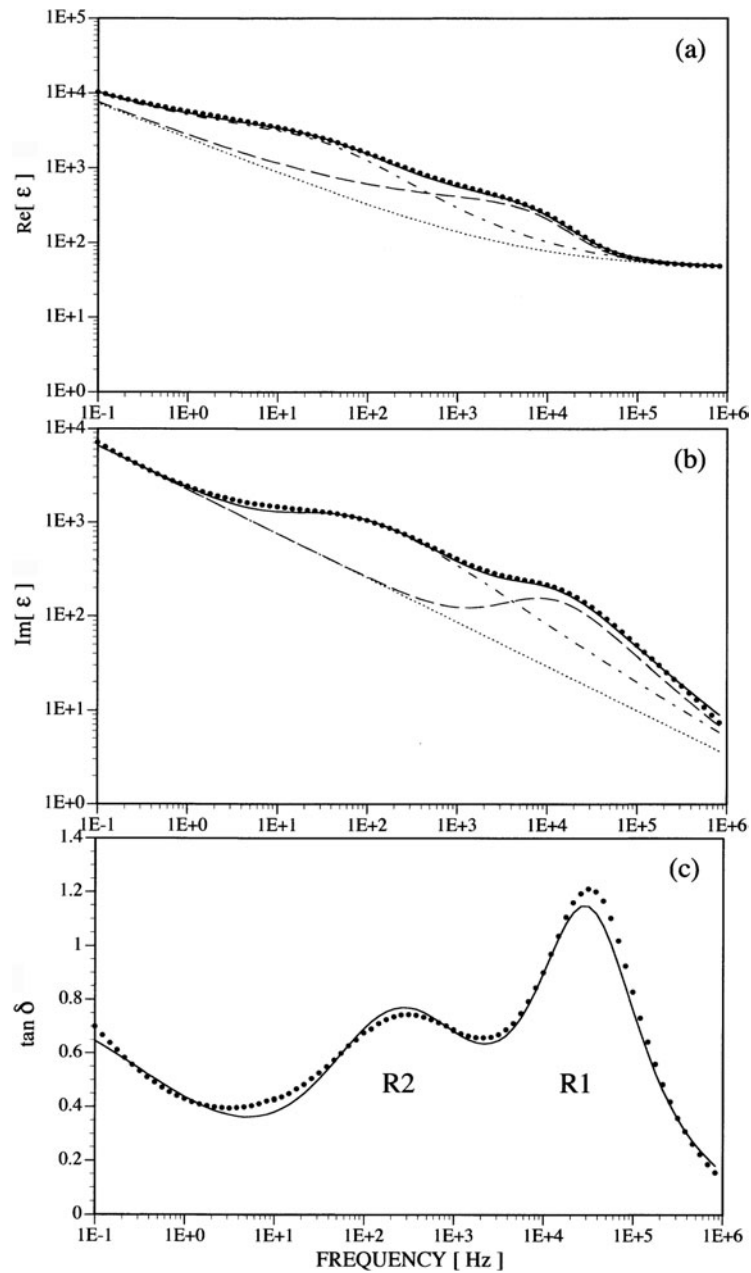


Figure 2. Comparison of experimental data (full circle): (a) ϵ' , (b) ϵ'' and (c) $\tan \delta$, with calculated values (solid curve) using equation (1) in SrZrO₃:Yb 2 mol% at 150 °C; dotted curve: $\epsilon_{\infty} + \sigma_0(\omega)^{-\gamma}$; dashed curves: $\frac{\Delta\epsilon_1}{[1+(i\omega\tau_1)^{\alpha_1}]^{\beta_1}}$ and $\frac{\Delta\epsilon_2}{[1+(i\omega\tau_2)^{\alpha_2}]^{\beta_2}}$.

that the ratio B/C is independent of Yb concentration, while A/C linearly increases with Yb. Therefore, the population of protons at state A shows a parabolic dependence on Yb concentration. Band A appears at high Yb concentration, which was also reported by Kreuer *et al* in BaCeO₃:Y [12]. In BaCeO₃:Y, the band at 1700 cm⁻¹ which corresponds to the band A

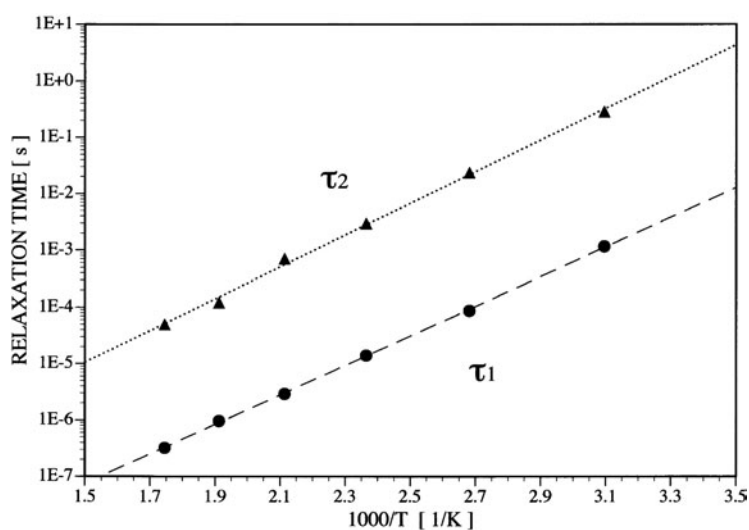


Figure 3. Temperature dependence of relaxation time τ_1 (full circle) and τ_2 (full triangle) of R1 and R2 in SrZrO₃:Yb 2 mol%, respectively.

in SrZrO₃:Yb was associated with the OH-stretching in the configuration Y–OH . . . O–Ce [12]. Considering the parabolic relation to the dopant concentration, one may assign the band A to the OH stretching associated with a dopant–dopant cluster such as Yb–OH . . . O–Yb.

On the other hand, Yugami *et al* [21] suggested four Gaussian bands in order to reproduce the bands B and C, and implied four types of fine states of the OH bonding, although the assignment for bands B and C is still unclear.

In order to understand the dielectric relaxation peaks (R1 and R2), the following models will be discussed. According to Hempelmann and Karmonik [10], the localized electric and elastic distortions produced by dopant ions can trap protons to form defect complexes. They suggested that the proton diffusion process was characterized as a combination of trapping and escape events at low-energy sites accompanied by a jump diffusion taking place over higher-energy sites. Based on this model, R1 and R2 can be assigned to the relaxations by trapped and free protons. Since the response of R1 is faster than that of R2 and the magnitude of $\Delta\epsilon$ (R2) is quite strong, about 10 000 for the sample containing more than 4 mol% of Yb, it is reasonable to suppose that R1 corresponds to a local reorientation of the Yb–OH dipole by a trapped proton and R2 to a space charge polarization, which is induced within the crystallites by free protons on the background of the effectively negative charged Yb ions. However, for a constant temperature, the average number of trapped and free protons, which is simply given by the Boltzmann distribution, depends on a total number of protons and a potential energy difference between low and high-energy sites. Since the total number of protons monotonically increases with an increase in Yb concentration from the IR measurement, the number of trapped protons at low-energy sites should increase. Thus, it is difficult to explain the decrease of the R1 relaxation strength $\Delta\epsilon$ (R1) with an increase in Yb concentration by using this model.

Here we propose a new model. As mentioned in the IR spectra, there are protons associated with the [YbO₆]⁺–[YbO₆]⁺ cluster. So we suppose that trapped protons contribute to both of the dielectric relaxations R1 and R2 with two types of proton–dopant association, and that free protons contribute to the conduction loss $\sigma_0(\omega)^{-\nu}$. If the magnitude of a single dipole moment is given by $p = er$, that of the pair cluster becomes $2p$. This cluster model assumes

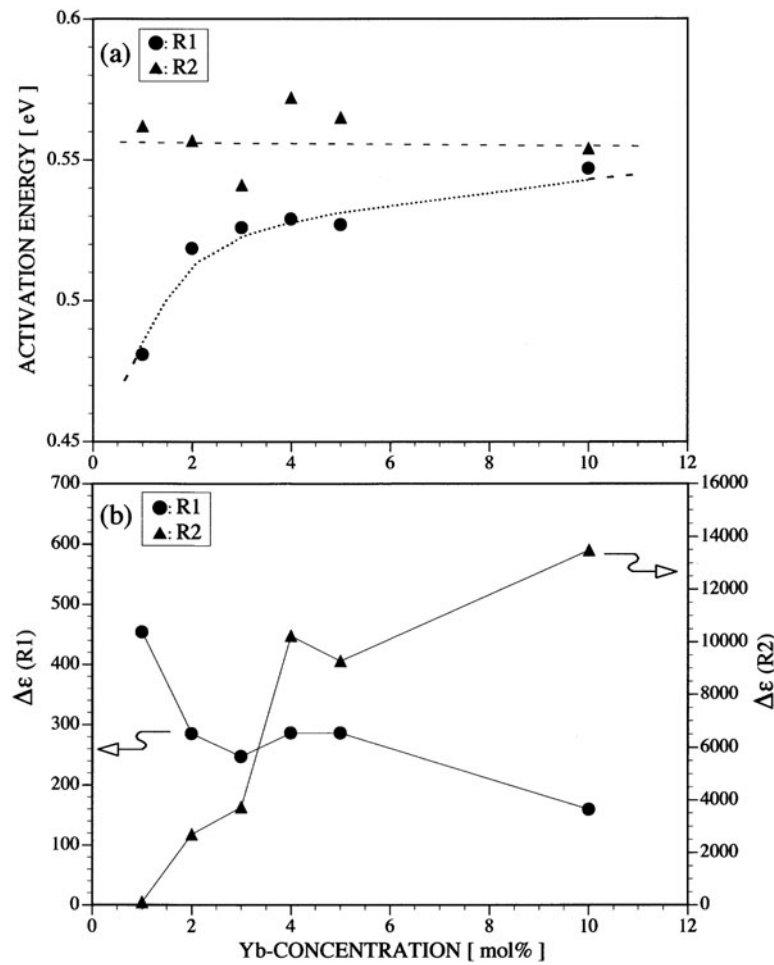


Figure 4. The Yb concentration dependence of (a) activation energy E_a and (b) relaxation strength $\Delta\epsilon$ of R1 (full circle) and R2 (full triangle) at 150 °C. The dotted and dashed curves are guides for the eye in (a).

that the reorientation of a single dipole is the origin of the relaxation R1 having weak relaxation strength and fast relaxation time, and that of the pair cluster dipole is the origin of the strong and slow R2 relaxation.

The clustering of Yb in SrZrO₃ is related to the miscibility of Yb₂O₃ and SrZrO₃. So we can apply the cluster variation method for a binary composition [23]. We consider only Zr and Yb ions distributed on a simple cubic lattice composed of M lattice points per unit volume, and the Sr and O ions are neglected for simplicity. The Zr and Yb ions are located at lattice points with the site probability x_1 and x_2 , respectively, and the pair probability of nearest neighbour ions i and j is denoted by y_{ij} , where $i, j = 1$ or 2 corresponding to Zr or Yb. Now we are interested in the disordered phase, so $y_{ij} = y_{ji}$. The x_i and y_{ij} are related by the following equation:

$$1 = \sum_{i=1}^2 x_i = \sum_{i,j=1}^2 y_{ij}, \quad \left(x_i = \sum_{j=1}^2 y_{ij} \right). \quad (2)$$

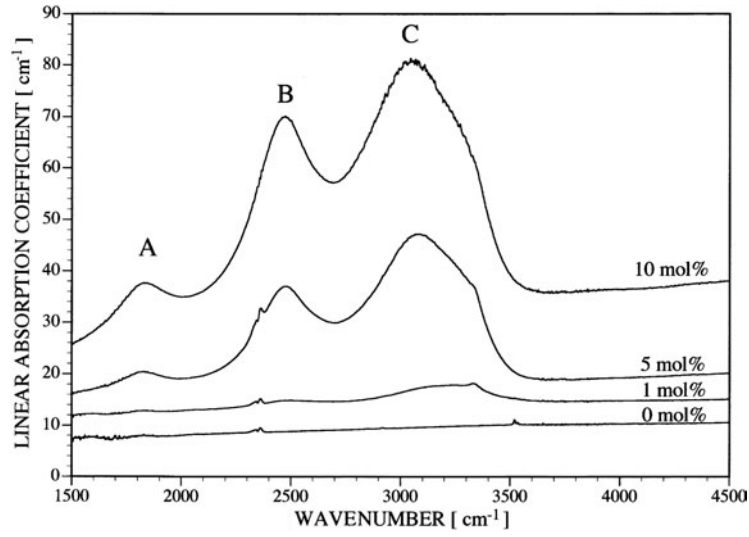


Figure 5. Infrared absorption spectra in the OH stretching region for $\text{SrZr}_{1-x}\text{Yb}_x\text{O}_3$ crystals of ($x = 0.0, 0.01, 0.05$ and 0.10) at room temperature.

Utilizing the pair approximation [23], the free energy is given by

$$F = M \left[3 \sum_{i,j} \phi_{ij} y_{ij} - k_B T \left\{ 5 \sum_i L(x_i) - 3 \sum_{i,j} L(y_{ij}) + 2 \right\} \right], \quad (3)$$

where $L(x) = x \ln x - x$, and ϕ_{ij} is the nearest neighbour interaction energy between i and j . The condition of the free energy minimum in equation (3) gives the equation

$$\phi + k_B T \ln \frac{y_{11}y_{22}}{y_{12}y_{21}} = 0, \quad \phi = \phi_{11} - 2\phi_{12} + \phi_{22}. \quad (4)$$

The number of isolated Yb ions (n_{iso}) and Yb–Yb pair clusters (n_{pair}) are expressed, respectively, as

$$\begin{aligned} n_{\text{iso}} &= M(y_{21})^6 \times (x_2)^{-5}, \\ n_{\text{pair}} &= 3My_{22}. \end{aligned} \quad (5)$$

An introduced proton is assumed to associate with the Yb ion for simplicity. The relaxation strength $\Delta\varepsilon$ of R1 and R2 can be evaluated using the simple Debye–Langevin model:

$$\begin{aligned} \Delta\varepsilon(\text{R1}) &= \frac{n_{\text{iso}}p^2}{3\varepsilon_0k_B T} = \frac{Mp^2}{3\varepsilon_0k_B T} \times (y_{21})^6 \times (x_2)^{-5}, \\ \Delta\varepsilon(\text{R2}) &= \frac{n_{\text{pair}}(2p)^2}{3\varepsilon_0k_B T} = \frac{M4p^2}{3\varepsilon_0k_B T} \times 3y_{22}. \end{aligned} \quad (6)$$

When an effective interaction energy ϕ is taken to be positive, the Zr–Yb pair is stable rather than Zr–Zr or Yb–Yb. In this case, the Zr and Yb ions are mixed homogeneously, and then it is possible to form an ordered phase at $x_2 > 1/6$ [24], while in the negative case, a phase separation will occur due to the clustering of Zr–Zr or Yb–Yb. Figure 7 shows the experimental results of $\Delta\varepsilon$ and the calculated ones using equation (6) with several values of ϕ for $M = 1.44 \times 10^{28} \text{ m}^{-3}$ at $T = 150^\circ\text{C}$ [25], where the dipole moment (p) is taken to be $p = er = e \times 42 \times 10^{-10} \text{ mC}$. Since the distance r between Yb–O is $r = 2.1 \times 10^{-10} \text{ m}$ at room temperature [26], this value (p) is twenty times as large as that of an ideal Yb–OH dipole. Such a large deviation

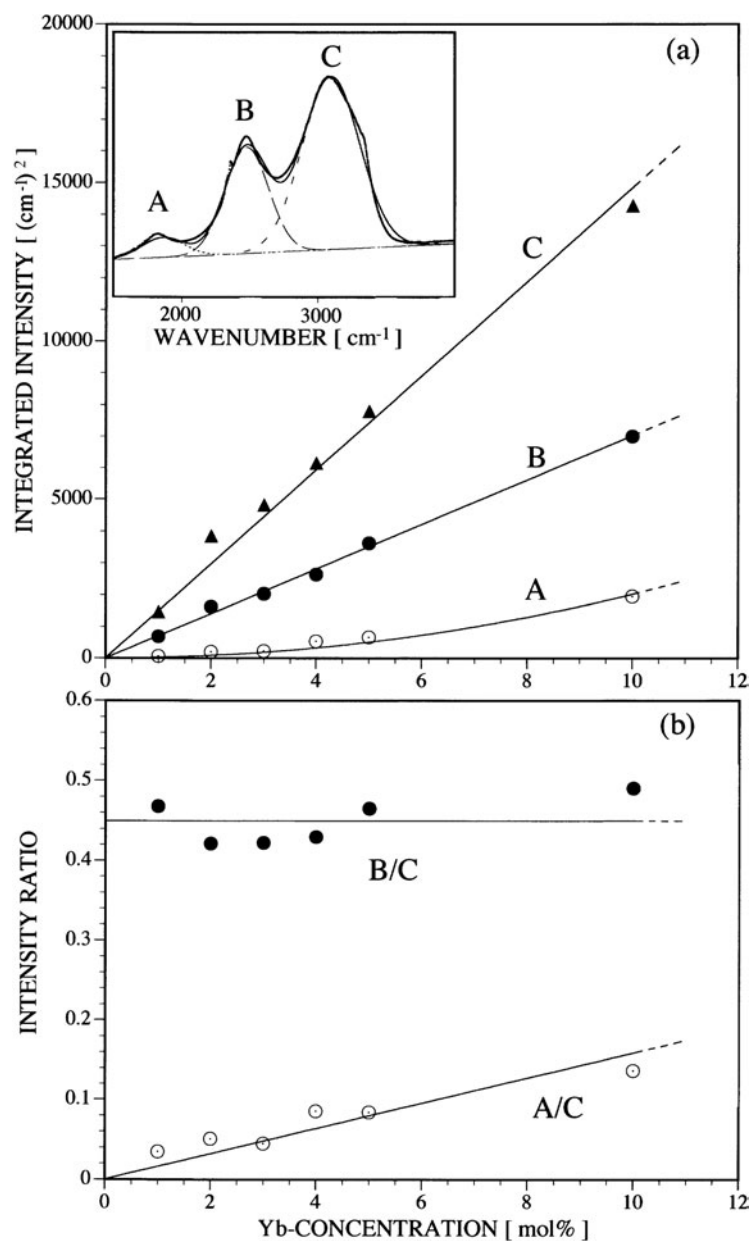


Figure 6. The Yb concentration dependence of (a) the integrated intensity of IR absorption bands A, B and C, and (b) the intensity ratios A/C and B/C. The solid curves are fitting results by linear and parabolic functions.

from the Debye–Langevin model has been previously reported, and an enhancement factor has been introduced, which is related to the dipole–dipole interaction or the local lattice distortion [27, 28]. Theoretical work was carried out by Vugmeister and Glinchuk [29] and by Stachiotti and Migoni [30]. Stachiotti and Migoni explained such an excess dipole moment by the interaction between a dipole and the surrounding lattice distortion [30]. In the case of off-centred Li in $\text{Li}_x\text{K}_{1-x}\text{TaO}_3$, the enhancement factor was theoretically estimated to

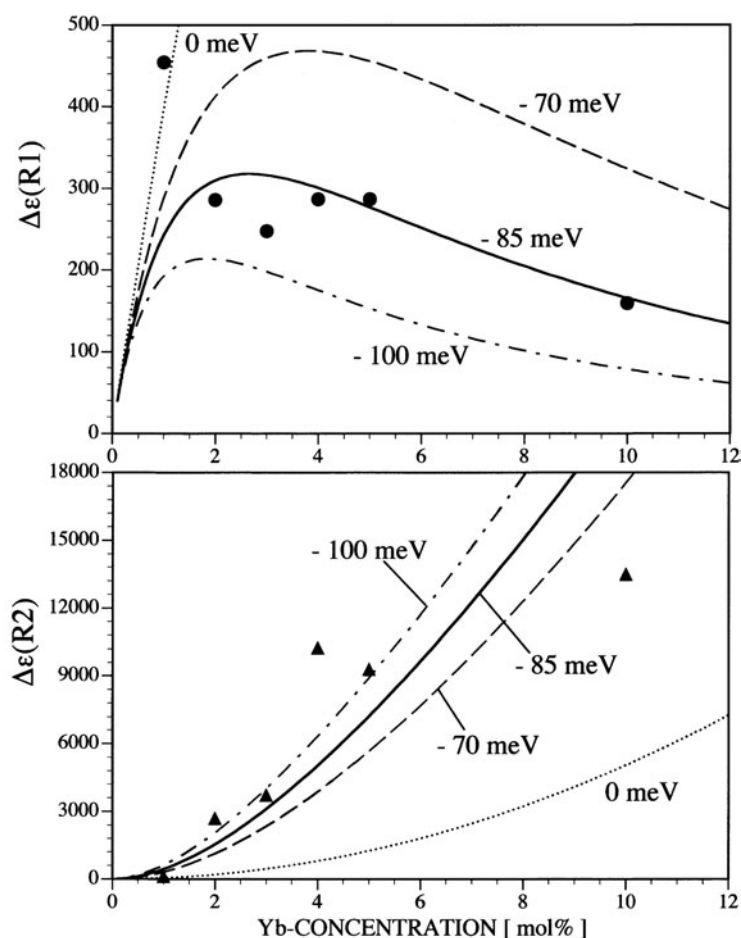


Figure 7. Comparison of the Yb concentration dependence of the relaxation strength $\Delta\epsilon(R1)$ and $\Delta\epsilon(R2)$ with various effective interaction energies ϕ .

be 4.5 (i.e. $p_{\text{eff}} = 4.5p_{\text{Li}}$) [30]. Experimentally, the enhancement factor for the off-centred Bi dipoles was also reported to be 20 or more in $\text{Sr}_{1-1.5x}\text{Bi}_x\text{TiO}_3$ [28]. Since the off-centred Yb was suggested by EXAFS measurement in $\text{SrZrO}_3:\text{Yb}$ [7], the effective dipole moment for Yb–OH can be considered to have such a large value $p_{\text{eff}} = 20p_{\text{Yb-OH}}$ from the present calculation. The attractive energy ($\phi < 0$) for Yb-clustering is evaluated at about -85 meV, as shown in figure 7. The magnitude of the nearest neighbour interaction energy is about the same as that calculated for Cu–Cu in CuBr (62 meV) [31].

This cluster model successfully explains that $\Delta\epsilon(R1)$ decreases, while the $\Delta\epsilon(R2)$ rapidly increases, with an increase in Yb concentration. The maximum compositional extent of the solid solution (e.g. around 15 mol% of Yb in SrZrO_3) may be due to the Yb-clustering.

5. Conclusion

Dielectric relaxation spectra were measured in the proton conductor $\text{SrZr}_{1-x}\text{Yb}_x\text{O}_3$ ($x = 0-0.1$). The compounds with more than 1 mol% Yb doping give rise to two well-defined relaxation peaks (R1 and R2). The Yb concentration dependence of the relaxation strength $\Delta\epsilon$ shows

a significant difference between R1 and R2. $\Delta\epsilon$ (R1) gradually decreases, while $\Delta\epsilon$ (R2) dramatically increases with an increase in Yb concentration.

The Yb concentration dependence of the IR spectra was investigated. There are at least three bands (designated A, B and C) for the OH-stretching. The population of protons at state A shows a parabolic dependence on Yb concentration. This implies that band A could be assigned to the –OH stretching associated with a Yb cluster such as Yb–OH...O–Yb.

The present study proposes a new model to understand the dielectric relaxations (R1 and R2). A free energy calculation for a mixture of Zr and dopant Yb ions reveals that the attractive energy ϕ to make clusters [YbO₆]²⁺–[YbO₆]²⁺... in SrZrO₃ is approximately –85 meV, and that the effective dipole p_{eff} is twenty times the magnitude of an ideal Yb–OH dipole. The relaxations R1 and R2 can be attributed to a reorientation of a single Yb–OH dipole and to Yb–OH dipoles associated with Yb-clusters, respectively.

Acknowledgments

The authors thank Professor M Maglione of the University of Bordeaux (France) for helpful discussions. The authors wish to acknowledge the contributions of Mr I Tanaka in the procedure of polishing the crystals. This work was supported by CREST of JST (Japan Science and Technology) and the Grant-in-Aid from ministry of education, culture, sports, science and technology of Japan.

References

- [1] Iwahara H, Esaka T, Uchida H and Maeda N 1981 *Solid State Ion.* **3/4** 359
- [2] Mitui A, Miyayama M and Yanagida H 1987 *Solid State Ion.* **22** 213
- [3] Scherban T, Lee W K and Nowick A S 1988 *Solid State Ion.* **28–30** 585
- [4] Shin S, Huagn H H, Ishigame M and Iwahara H 1990 *Solid State Ion.* **40/41** 910
- [5] Yajima T, Suzuki H, Yogo T and Iwahara H 1992 *Solid State Ion.* **51** 101
- [6] Liu J F and Nowick A S 1992 *Solid State Ion.* **50** 131
- [7] Kamishima O, Ohta K, Chiba Y and Hattori T 2001 *J. Phys.: Condens. Matter* **13** 2455
- [8] Howard C J, Knight K S, Kennedy B J and Kisi E H 2000 *J. Phys.: Condens. Matter* **12** L677
- [9] Kamishima O, Hattori T, Ohta K, Chiba Y and Ishigame M 1999 *J. Phys.: Condens. Matter* **11** 5355
- [10] Hempelmann R and Karmonik Ch 1996 *Phase Transit.* **58** 175
- [11] Ishii T and Ichigozaki A 2004 *J. Phys. Soc. Japan* **73** 130
- [12] Kreuer K D, Munch W, Ise M, He T, Fuchs A, Traub U and Maier J 1997 *Ber. Bunsenges. Phys. Chem.* **101** 1344
- [13] Zimmermann L, Bohn H G, Schilling W and Syskakis E 1995 *Solid State Ion.* **77** 163
- [14] Zimmermann L, Baush S, Bohn H G and Schilling W 1996 *J. Physique IV* **6** C8 699
- [15] Du Y 1994 *J. Phys. Chem. Solids* **55** 1485
- [16] Kosacki I, Schoonman J and Balkanski M 1992 *Solid State Ion.* **57** 345
- [17] Havriliak S and Negami S 1967 *Polymer* **8** 161
- [18] Kawamura J, Stato R, Mishina S and Shimoji M 1987 *Solid State Ion.* **25** 155
- [19] Iwahara H, Yajima T and Ushida H 1994 *Solid State Ion.* **70/71** 267
- [20] Schober T, Friedrich J and Condon J B 1995 *Solid State Ion.* **77** 175
- [21] Yugami H, Shibayama Y, Hattori T and Ishigame M 1995 *Solid State Ion.* **79** 171
- [22] Kreuer K D 1997 *Solid State Ion.* **97** 1
- [23] Kikuchi R 1951 *Phys. Rev.* **81** 988
- [24] Ishii T and Kawamura J 1998 *J. Phys. Soc. Japan* **67** 3517
- [25] Ligny D and Richet P 1996 *Phys. Rev. B* **53** 3013
- [26] Ahtee A, Ahtee M, Glazer A M and Hewat A W 1976 *Acta Crystallogr. B* **32** 3243
- [27] Maglione M, Bohmer R, Loidl A and Hochli U T 1989 *Phys. Rev. B* **40** 11441
- [28] Ang C and Yu Z 2000 *Phys. Rev. B* **61** 11363
- [29] Vugmeister B E and Glinchuk M D 1990 *Rev. Mod. Phys.* **62** 993
- [30] Stachiotti M G and Migoni R L 1990 *J. Phys.: Condens. Matter* **2** 4341
- [31] Ishii T and Kamishima O 1999 *J. Phys. Soc. Japan* **68** 3580